Carrier photogeneration of *N*-phenylcarbazole doped poly(bisphenol A carbonate) film

Naoto Tsutsumi, Masahide Yamamoto* and Yasunori Nishijima
Department of Polymer Chemistry, Faculty of Engineering, Kyoto University, Sakyo-ku, Kyoto 606, Japan
(Received 14 September 1987; revised 7 December 1987; accepted 8 January 1988)

The carrier photogeneration mechanism of *N*-phenylcarbazole (PhCz) doped poly(bisphenol A carbonate) film with 2,6-dimethyl-*p*-benzoquinone (MQ) as an electron acceptor was investigated. The carrier generation efficiency, η, was measured by a xerographic technique. The extrinsic carrier generation efficiency, η_e, was calculated from η and fluorescence quenching data. The large increase of η_e with increasing PhCz is attributed to excitation energy migration to the acceptor site MQ. The probability of free carrier formation at the acceptor site, $A_e(E)$, is nearly constant, $\approx 1.5 \times 10^{-3}$. The electric field dependence of η_e was analysed by an Onsager plot. The initial separation distance of the ion pair, r_0, is 1.8–2.0 nm. The slight increase of $A_e(E)$ and r_0 with increasing PhCz concentration seems to be caused by enhanced escape probability from the geminate recombination due to hole migration.

(Keywords: carrier photogeneration; phenylcarbazole-doped poly(bisphenol A carbonate); xerographic technique; fluorescence quenching; Onsager plot)

INTRODUCTION

The photoconductivity of polymer systems doped with various low molecular weight compounds (molecularly doped polymer systems) has been investigated extensively for the carrier photogeneration process[1-5] and for the carrier transport process[1,6-11] For the carrier photogeneration process, excimer-forming sites work as trapping sites of the excitation energy and suppress the carrier generation efficiency. For the carrier transport process, excimer-forming sites also work as trapping sites of charge carriers[9,11]. To understand the mechanism of photoconductivity in polymer systems, it is desirable to study systems having no excimer-forming sites[12]. Some carbazole derivative doped poly(bisphenol A carbonate) (PC) systems, such as *N*-phenylcarbazole (PhCz) doped PC film[10,13] and *trans*-1,2-biscarbazolylcyclobutane doped PC film[11], have been found to have no excimer-forming sites.

There are several reports on carrier photogeneration for aromatic amine (e.g. triphenylamine[3] and *N*-isopropylcarbazole[5]) doped polymer systems. In these studies, it is shown that an increase of aromatic amine concentration increases the carrier generation efficiency, but the dispersed state of dopants in polymer films and the nature of carrier generation sites have not been clarified.

In the work reported in this paper, the carrier photogeneration mechanism of *N*-phenylcarbazole doped poly(bisphenol A carbonate) films was investigated by adding 2,6-dimethyl-*p*-benzoquinone (MQ) as an acceptor. Extrinsic photogeneration efficiency was estimated by the combination of a xerographic technique with a fluorescence quenching method. In this system, excimer-forming sites are not produced even at a high concentration of PhCz of 2.4 mmol cm^{-3} (48 wt%) and an extrinsic carrier generation site, MQ, is dispersed in the system. *Figure 1* shows the structural formulae and chemical symbols used in this paper.

EXPERIMENTAL

Sample preparation

Poly(bisphenol A carbonate) (PC) (Polyscience, Merlon, M-40) was purified by re-precipitation in methanol from dichloromethane solution. *N*-Phenylcarbazole (PhCz) (Aldrich Chemical Company Inc.) and 2,6-dimethyl-*p*-benzoquinone (MQ) (Aldrich Chemical Company Inc.) were recrystallized from ethanol and cyclohexane, respectively. Thin film was cast on an aluminium plate from a dichloromethane solution of PC at ambient temperature in which PhCz and MQ were present at different ratios. Film thickness was determined by using the equation

$$\text{film thickness} = \frac{\text{polymer weight}}{\text{area} \times \text{density}}$$

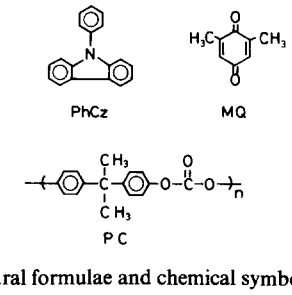

Figure 1 Structural formulae and chemical symbols used in this work

* To whom correspondence should be addressed

0032-3861/88/091655-04$03.00

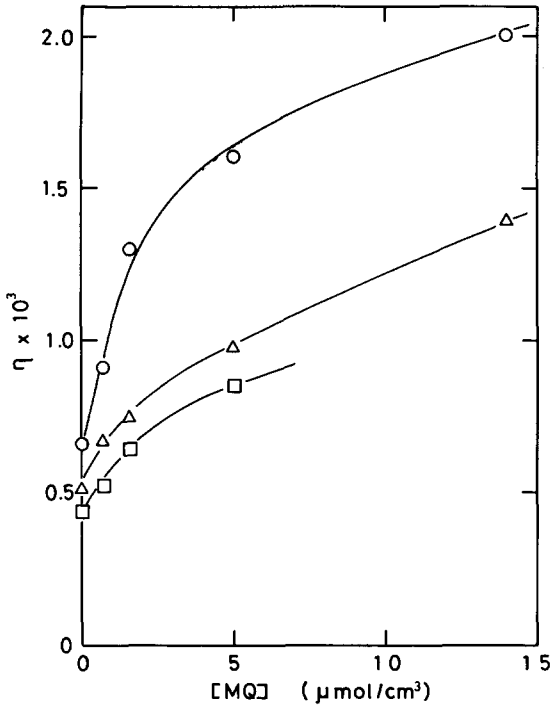

Figure 2 Dependence of carrier generation efficiency, η, on MQ concentration for various concentrations of PhCz (mmol cm^{-3}): ○, 2.4; △, 1.2; □, 0.81

The density of the films was determined by using a density gradient column to be in the range 1.202–1.209 g cm^{-3}. Film thickness was in the range 2.0–4.0 μm.

No crystallization was recognized by differential scanning calorimetry (d.s.c.) or with a polarizing microscope.

Fluorescence measurement

Fluorescence spectra were measured at the front surface of a sample film in air with a calibrated Shimadzu RF-502 spectrofluorophotometer at ambient temperature.

Carrier generation measurement

Carrier generation efficiency, η, was measured by a photo-induced discharge technique (a xerographic measurement)[14]. The sample, a photoconductive polymer, was passed under the corona discharge device of 6 kV tungsten wire and a positive charge was deposited on the surface of the photoconductive polymer. After the sample had been charged, it was put under the transparent probe of an electrometer follower (Monroe Model 145) and the surface potential $V(t)$ was monitored. A model 145 electrometer follower is basically a solid-state differential operational amplifier employing metal–oxide–semiconductor field effect transistors (MOSFETs) for its input stage. The sample was then illuminated with the excitation light through the transparent probe of the electrometer. The electrons produced by the excitation light neutralize the positive charges on the surface of the sample, and the hole carriers are transported through the sample.

The electrometer was calibrated by a sample of known potential under the transparent probe. Excitation light was provided by a 500 W xenon lamp (Ushio) through a grating monochromator (slit width 10 nm) equipped with a shutter. The absolute intensity of light at 340 nm was measured by using actinometry[15] as 2.5×10^{14} photons $cm^{-2}\ s^{-1}$.

Under the emission-limited discharge condition, the carrier generation efficiency, η, was calculated by using the following equation:

$$\eta = -\varepsilon\varepsilon_0/(eI_0L)(dV/dt)_{t=0} \quad (1)$$

where ε is the dielectric constant of the sample, ε_0 is the permittivity of free space, e is electronic charge, I_0 is the incident photon flux, L is the sample thickness, and $(dV/dt)_{t=0}$ is the time derivative of surface potential at $t=t_0$.

RESULTS AND DISCUSSION

The fluorescence spectrum showed only emission from the monomer state; excimer emission was not observed even at a high concentration of PhCz, 2.4 mmol cm^{-3} (48 wt%). The fluorescence decay curves measured in the wavelength range 370–390 nm were single exponential curves: $\tau = 8.6$ ns at [PhCz] = 0.81 mmol cm^{-3} (16 wt%)[13]. The intensity of monomer emission of PhCz is quenched by the addition of a small amount of acceptor (for the quantitative result, see *Figure 4*). This indicates that the excitation energy of PhCz migrates among PhCz residues and transfers to the acceptor site MQ.

Figure 2 shows the MQ concentration dependence of the carrier generation efficiency, η, at 340 nm excitation for various concentrations of PhCz. The carrier generation efficiency increases with increasing MQ concentration at a fixed PhCz concentration and also with increasing PhCz concentration at a fixed MQ concentration. Here, MQ concentration is $\approx 1/1000$ PhCz concentration. The enhancement of the carrier generation efficiency, η, with increasing MQ concentration is due to the increase of carrier generation sites. The increase of η with increasing PhCz concentration is mainly due to the enhancement of excitation energy migration.

Carrier generation efficiency, η, has been analysed from fluorescence quenching data. *Figure 3* shows the scheme for the carrier generation process of PhCz doped PC film with MQ as an acceptor (PhCz–MQ/PC). Since the glass transition temperature for the PhCz/PC system is higher than ambient[10], translational diffusion of added guest molecules, PhCz and MQ, is frozen in the PC matrix. Hence the excitation energy migrates among PhCz molecules and reaches the acceptor site MQ. Electron transfer from PhCz* to MQ then produces the ion pair ($PhCz^+ \cdots MQ^-$). The free carrier is generated from this ion pair with the assistance of the electric field. The electron transfer process from PhCz* to the acceptor site MQ competes with that from PhCz* to an unknown acceptor site, A. In *Figure 3*, k_q and k_i are the rate constants for excited state quenching by acceptor MQ

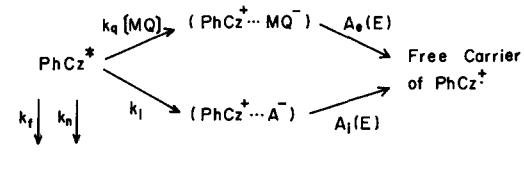

Figure 3 Carrier photogeneration process for PhCz–MQ/PC system. A is an unknown acceptor

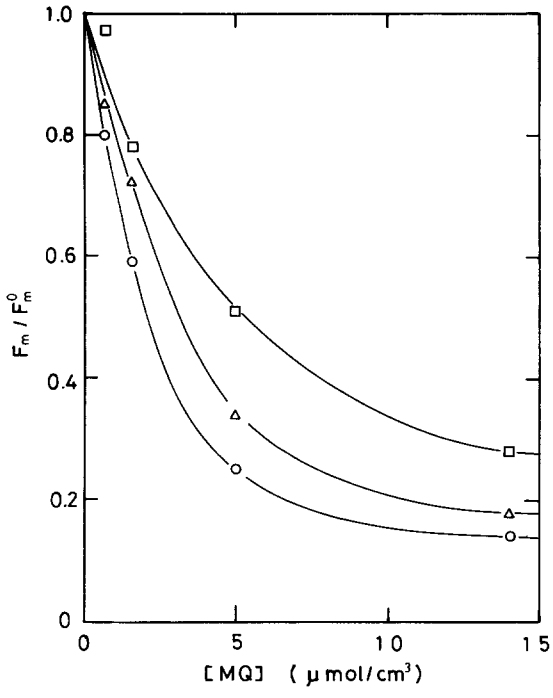

Figure 4 Plot of F_m/F_m^0 *versus* MQ concentration for various concentrations of PhCz (mmol cm^{-3}): ○, 2.4; △, 1.2; □, 0.81

and by an unknown acceptor, A, respectively; k_f and k_n are the rate constants of fluorescence and non-radiative processes, respectively, for PhCz*; and $A_i(E)$ and $A_e(E)$ are the probability of free carrier formation from the carrier generation site of an unknown acceptor, A, and from acceptor MQ, respectively. A detailed investigation into energy migration and transfer to the acceptor site MQ is reported elsewhere[13].

In the present system, the observed carrier generation efficiency, η, is the sum of the carrier generation efficiency of an unknown acceptor, A, η_i, and of the doped acceptor MQ, η_e:

$$\eta = \eta_i + \eta_e \tag{2}$$

According to the scheme in *Figure 3*, η_i and η_e can be written as:

$$\eta_i = [k_i/(k + k_q[MQ])]A_i(E) \tag{3}$$

$$\eta_e = [k_q[MQ]/(k + k_q[MQ])]A_e(E) \tag{4}$$

where $k = k_f + k_n + k_i$.

When MQ is zero, the observed carrier generation efficiency, η_i^0, is expressed as

$$\eta_i^0 = (k_i/k)A_i(E) \tag{5}$$

Then η_e is calculated from equations (2), (3) and (5):

$$\eta_e = \eta - [k/(k + k_q[MQ])]\eta_i^0 \tag{6}$$

The value of $k/(k + k_q[MQ])$ is obtained by the fluorescence quenching of monomer emission:

$$F_m/F_m^0 = k/(k + k_q[MQ]) \tag{7}$$

where F_m^0 and F_m are the fluorescence intensities of PhCz in the absence of MQ and in the presence of MQ, respectively.

Then:

$$\eta_e = \eta - (F_m/F_m^0)\eta_i^0 \tag{8}$$

and

$$\eta_e = (1 - F_m/F_m^0)A_e(E) \tag{9}$$

Figure 4 shows plots of F_m/F_m^0 against [MQ] for various concentrations of PhCz. Then the η_e value was calculated from equation (8) and *Figures 2* and *4*. *Figure 5* shows the relation between η_e and MQ concentration. At a fixed PhCz concentration, η_e increases with increasing MQ concentration, and at a fixed MQ concentration, η_e increases with increasing PhCz concentration. The probability of free carrier formation from the MQ site, $A_e(E)$, is obtained from equation (9) and *Figures 4* and *5*. *Figure 6* shows the relation between $A_e(E)$ and PhCz concentration. $A_e(E)$ is nearly constant, $\approx 1.5 \times 10^{-3}$, but slightly increases with PhCz concentration. The increase of $A_e(E)$ with increasing PhCz concentration seems to be

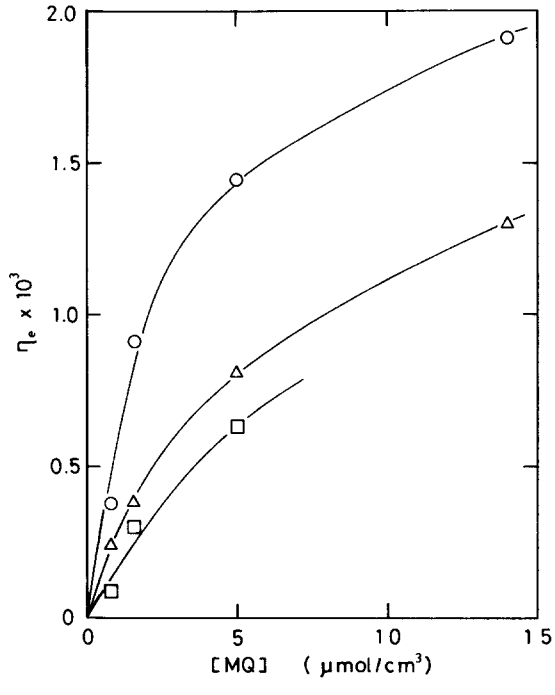

Figure 5 Plot of η_e *versus* MQ concentration for various concentrations of PhCz (mmol cm^{-3}): ○, 2.4; △, 1.2; □, 0.81

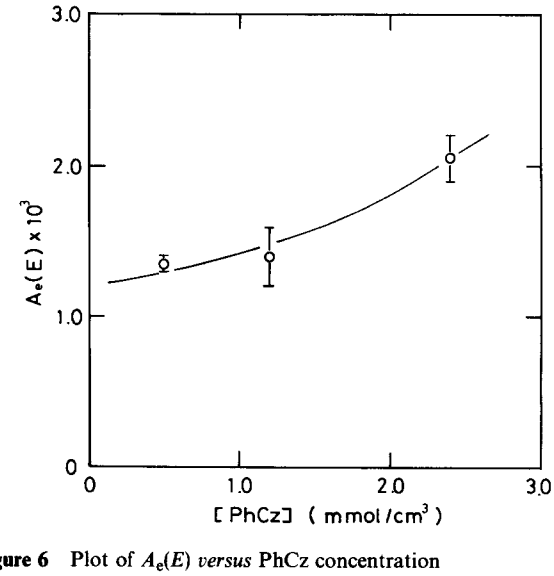

Figure 6 Plot of $A_e(E)$ *versus* PhCz concentration

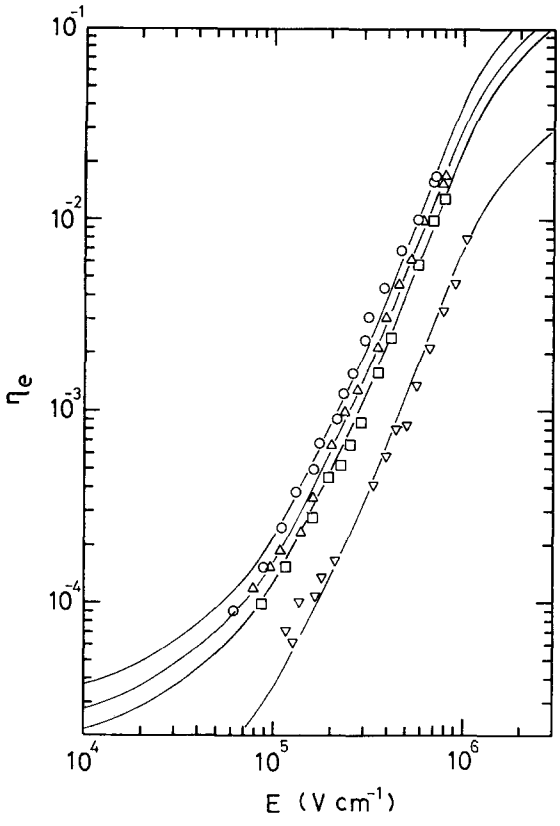

Figure 7 Dependence of η_e on electric field at [PhCz] = 2.4 mmol cm^{-3} for various concentrations of MQ (μmol cm^{-3}): ○, 14; △, 5.0; □, 1.6; ▽, 0.71. The solid lines are Onsager curves for $r_0 = 2.0$ nm, with $\Phi_0 = 0.42$, 0.24, 0.18 and 0.05 for [MQ] = 14, 5.0, 1.6 and 0.71 μmol cm^{-3}, respectively

caused by enhanced escape probability from the geminate recombination due to hole migration.

The electric field dependent curves of the carrier generation efficiency at various concentrations of PhCz and MQ were analysed by an Onsager plot[16-19]. For the process of free carrier formation, the ion pair thermalizes with an initial separation distance (r_0) and the hole (PhCz cation radical) escapes from the geminate recombination with the counter ion (MQ anion radical). *Figure 7* shows a typical fitting curve for [PhCz] = 2.4 mmol cm^{-3}. The primary quantum yields, Φ_0, of 0.05, 0.18, 0.24 and 0.42 with an initial distance $r_0 = 2.0$ nm were obtained for [MQ] = 0.71, 1.6, 5.0 and 14 μmol cm^{-3}, respectively. The values of r_0 and Φ_0 are 1.8 nm and 0.08, respectively, for [PhCz] = 0.81 mmol cm^{-3}, 1.8 nm and 0.10 for [PhCz] = 1.2 mmol cm^{-3}, 2.0 nm and 0.18 for [PhCz] = 2.4 mmol cm^{-3} under a fixed [MQ] = 1.6 μmol cm^{-3}. The value of r_0 tends to increase slightly with increasing PhCz concentration. This result is consistent with the fact that $A_e(E)$ tends to increase with increasing PhCz concentration. This seems to indicate that at a higher concentration of PhCz hole migration among neighbouring PhCz residues becomes easier, and induces the enhancement of escape probability from the geminate recombination. The values of Φ_0 are a few times smaller than the degree of fluorescence quenching for the same samples. It seems that a fraction of the ion pairs formed by the photo-induced electron transfer recombines before the formation of thermalized ion pairs, i.e. without being subject to the electric field.

CONCLUSION

The enhancement of carrier photogeneration efficiency with increasing PhCz concentration is mainly attributed to the increase of energy migration to the acceptor site MQ; the increase of carrier generation efficiency with increasing MQ concentration is due to the increase of carrier generation sites. The probability of free carrier formation in the acceptor site MQ, $A_e(E)$, and the initial separation distance of the ion pair, r_0, tend to increase with increasing PhCz concentration. This suggests that hole migration among neighbouring PhCz residues becomes easier with increasing PhCz concentration and induces an increased escape probability for the geminate recombination.

ACKNOWLEDGEMENT

This work was supported by Grant-in-aid for Scientific Research no. 59470089, from the Ministry of Education, Science and Culture, Japan.

REFERENCES

1 Mort, J., Pfister, G. and Grammatica, S. *Solid State Commun.* 1976, **18**, 693
2 Grammatica, S. and Mort, J. *J. Chem. Phys.* 1977, **67**, 5628
3 Borsenberger, P. M., Contois, L. E. and Hoesterey, D. C. *J. Chem. Phys.* 1978, **68**, 637
4 Borsenberger, P. M., Contois, L. E. and Hoesterey, D. C. *Chem. Phys. Lett.* 1978, **56**, 574
5 Borsenberger, P. M., Contois, L. E. and Ateya, A. I. *J. Appl. Phys.* 1979, **50**, 914
6 Pfister, G. *Phys. Rev. B* 1977, **16**, 3676
7 Borsenberger, P. M., Mey, W. and Chowdry, A. *J. Appl. Phys.* 1978, **49**, 273
8 Pai, D. M., Yanus, J. F., Stolka, M., Renfer, D. and Limburg, W. W. *Phil. Mag. B* 1983, **48**, 505
9 Yokoyama, M., Akiyama, K., Yamamori, N., Mikawa, H. and Kusabayashi, S. *Polym. J.* 1985, **17**, 545
10 Tsutsumi, N., Yamamoto, M. and Nishijima, Y. *J. Appl. Phys.* 1986, **59**, 1557
11 Tsutsumi, N., Yamamoto, M. and Nishijima, Y. *J. Polym. Sci., Polym. Phys. Edn.* 1987, **25**, 2139
12 Ito, S., Yamashita, K., Yamamoto, M. and Nishijima, Y. *Chem. Phys. Lett.* 1985, **117**, 171
13 Tsutsumi, N., Yamamoto, M. and Nishijima, Y. in preparation
14 Mort, J. and Chen, I. in 'Applied Solid State Science', Academic Press, New York, 1975, p. 69
15 Hatchard, C. G. and Parker, C. A. *Proc. Roy. Soc. Lond.* 1956, **253A**, 518
16 Onsager, L. *Phys. Rev.* 1938, **54**, 554
17 Mozumder, A. *J. Chem. Phys.* 1974, **60**, 4300
18 Mozumder, A. *J. Chem. Phys.* 1974, **60**, 4305
19 Pai, D. M. and Enck, R. C. *Phys. Rev. B* 1975, **11**, 5163